# NF-κB regulation of endothelial cell function during LPS-induced toxemia and cancer

Tatiana Kisseleva,[1,2] Li Song,[1] Marina Vorontchikhina,[3] Nikki Feirt,[3] Jan Kitajewski,[3] and Christian Schindler[1,2]

[1]Department of Microbiology, [2]Department of Medicine, and [3]Department of Pathology, College of Physicians and Surgeons, Columbia University, New York, New York, USA.

**The transcription factor NF-κB is an important regulator of homeostatic growth and inflammation. Although gene-targeting studies have revealed important roles for NF-κB, they have been complicated by component redundancy and lethal phenotypes. To examine the role of NF-κB in endothelial tissues, Tie2 promoter/enhancer–IκBα$^{S32A/S36A}$ transgenic mice were generated. These mice grew normally but exhibited enhanced sensitivity to LPS-induced toxemia, notable for an increase in vascular permeability and apoptosis. Moreover, B16-BL6 tumors grew significantly more aggressively in transgenic mice, underscoring a new role for NF-κB in the homeostatic response to cancer. Tumor vasculature in transgenic mice was extensive and disorganized. This correlated with a marked loss in tight junction formation and suggests that NF-κB plays an important role in the maintenance of vascular integrity and response to stress.**

## Introduction

Vascular endothelium, which comprises a monolayer of more than ten trillion ECs, represents a dynamic interface between the circulatory system and nonvascular tissues (reviewed in ref. 1). Of note, endothelium is far more than a barrier, playing critical roles in regulating the levels of cellular metabolites, vascular tone and hemostasis, as well as the ingress and egress of leukocytes. Because of their capacity to direct leukocyte traffic through controlled expression of homeostatic and inflammatory mediators (e.g., adhesion molecules, chemokines, and cytokines), ECs play a critical role in regulating inflammation (1–4). ECs also actively participate in the processes of angiogenesis, vascular remodeling, and tumorigenesis (1, 5–7).

Systemic viral and bacterial infections are associated with activation of an innate immune response that includes the expression of proinflammatory cytokines and chemokines. Some of these inflammatory cytokines (e.g., TNF-α, IL-1) have profound effects on endothelial function, including their regulation of vascular tone, permeability, and leukocyte diapedesis (1, 8). During times of overwhelming sepsis, these inflammatory mediators trigger septic shock, a syndrome associated with EC failure and death (1, 4, 9). Likewise, "successful" tumors also appear to have the capacity to manipulate endothelial function, as they promote their own spread and become vascularized (5, 10).

The endothelium regulates these dynamic interactions with the environment through intracellular signaling cascades. As is the case in many other tissues, JNK- and NF-κB–dependent pathways play an important role during the endothelial response to inflammatory stress (9, 11–13). In resting cells, NF-κB (i.e., RelA/p65 and NFkB1/p50) associates with IκBα, a negative regulator, forming an inactive complex. Upon stimulation with an appropriate ligand (e.g., TNF-α, IL-1, LPS), IκBα serines 32 and 36 become phosphorylated, and the protein is targeted for degradation. This releases the p65:p50

dimer, freeing it to translocate into the nucleus, where it induces the expression of target genes. Mutation of these 2 critical serines (i.e., IκBα$^{S32A/S36A}$) serves to block IκBα degradation and renders p65:p50 functionally inactive (12, 14–16). This "superinhibitory" mutant of IκBα, referred to as sIκBα, has been successfully exploited to explore the role of classical NF-κB signaling in immunity, inflammation, and tumorigenesis (12, 14, 16, 17). Moreover, these studies have revealed the critical role this pathway plays in antagonizing apoptosis (18). Gene-targeting studies, which have validated some observations about NF-κB function, have been hampered by redundancy within the family of NF-κB transcription factors and embryonic lethal phenotypes (12, 19, 20).

To explore the role NF-κB signaling plays in the dynamic regulation of endothelium, the Tie2 promoter/enhancer was exploited to direct expression of sIκBα to ECs in transgenic mice (21). Despite endothelial inhibition of NF-κB signaling, these mice grew and reproduced normally. They also exhibited a normal pattern of vascular development. However, transgenic mice exhibited enhanced sensitivity toward LPS-induced toxemia and metastatic melanoma. Size-matched tumors that grew in transgenic mice exhibited a significant increase in vascular density. Moreover, these blood vessels were disorganized and revealed a significant decrease in the structural integrity of endothelial tight junctions (TJs), highlighting an important role for NF-κB in homeostatic vascular stability. These results highlight 2 critical functions for endothelial NF-κB. First, NF-κB provides an important survival signal for the acute stress associated with LPS-induced toxemia. Second, NF-κB helps maintain a normal but dynamic endothelial barrier function. These studies provide new insights into the nature of tumor cell/endothelial interactions and suggest a role for endothelial NF-κB in restricting tumorigenesis.

## Results

*Generation and initial characterization of sIκBα-transgenic mice.* To investigate the role of NF-κB signaling in endothelial cell function in vivo, the Tie2 enhancer/promoter was exploited to drive the expression of a dominant interfering sIκBα mutant (IκBα$^{S32A/S36A}$) in vascular tissues (Figure 1A; ref. 14). Although this enhancer/promoter is known to effectively direct endothelial expression,
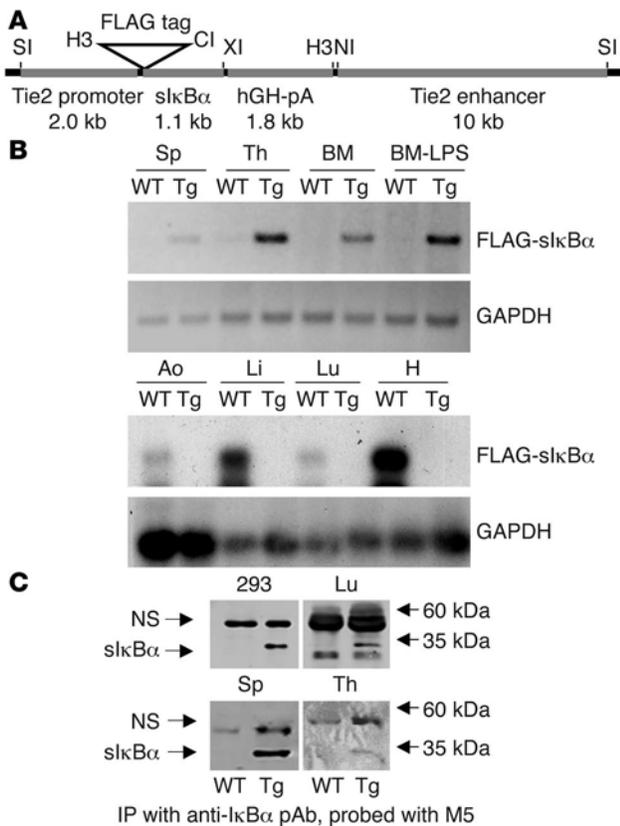
**Figure 1**

Generation of transgenic mice. (**A**) The transgenic construct consisted of the Tie2 promoter, dominant negative FLAG-tagged sIkBα$^{S32A/S36A}$, hGH polyadenylation cassette (hGH-pA), and the Tie2 enhancer. Restriction sites for SalI (SI), HindIII (H3), ClaI (CI), XbaI (XI), and NcoI (NI) are shown. (**B**) RT-PCR analysis for sIkBα expression in RNA from transgenic (line 2) and WT heart (H), lung (Lu), liver (Li), aorta (Ao), spleen (Sp), thymus (Th), and BM. The PCR product was visualized either by UV fluorescence (upper 2 panels) or hybridization with IkBα or GAPDH [$^{32}$P]dCTP-radiolabeled probes (lower 2 panels). One set of BM was harvested from mice 7 days after LPS stimulation (2 μg/g). (**C**) IkBα and sIkBα protein expression was evaluated by a sensitive immunoblotting (anti-FLAG M5 mAb; Sigma-Aldrich)/ immunoprecipitation (IkBα polyclonal Ab [pAb]; Santa Cruz Biotechnology Inc.) assay in lung, splenic, and thymic extracts prepared from transgenic mice (line 4). Extracts prepared from HEK 293T cells transiently transfected with the sIkBα expression vector served as a positive control. A nonspecific (NS) band (recognized by M5 mAb) and size standards are indicated.

more recent studies have revealed additional expression in hematopoietic tissues (21–23). An aminoterminal FLAG epitope tag was included on sIkBα to facilitate distinguishing the transgene from endogenous IkBα. Four Tie-Tg lines were generated, each with approximately 15–20 copies of an integrated transgene (Supplemental Figure 1A; supplemental material available online with this article; doi:10.1172/JCI27392DS1). Expression of the FLAG-sIkBα transgene was first confirmed by transgene-specific RT-PCR in several well-vascularized tissues, including spleen, thymus, bone marrow, lung, and aorta (Figure 1B). The FLAG-sIkBα protein was detected by immunoblotting after IkBα immunoprecipitation in extracts from transgenic lung, spleen, and thymus (Figure 1C). Since no significant differences were found among the 4 transgenic lines, in either sIkBα expression or response to LPS (see also below), lines 2 and 4 were selected for further study.

*Transgenic mice are highly susceptible to LPS-induced septic shock.* Previous studies have suggested that NF-κB directs an antiapoptotic response in TNF-α–treated human umbilical vein ECs (9, 24, 25). Therefore, we hypothesized that transgenic ECs would be defective in their response to LPS, which stimulates a robust increase in circulating levels of TNF-α (and IL-1β; refs. 26, 27). When 8-week-old transgenic mice were challenged with a sublethal dose of to LPS (8 μg/g), each of the 4 Tie-Tg lines rapidly developed symptoms consistent with sepsis (e.g., lethargy, diarrhea, and ocular discharge; data not shown), whereas nontransgenic littermate controls did not. A more extensive analysis of Tie-Tg lines 2 and 4 determined that they rapidly died within 60 hours after LPS challenge, whereas 95% of control mice survived (Figure 2A). Postmortem evaluation of transgenic mice revealed extensive organ failure (e.g., liver, lungs, and spleen; Supplemental Figure 2A and data not shown).

To more carefully explore the enhanced LPS susceptibility of Tie-Tg mice, lines 2 and 4 were injected with a lower dose of LPS (i.e., 2 μg/g), which did not cause death. A pathological survey of these mice revealed a significant initial increase in spleen size in both control and transgenic mice. But over the next 7 days, as WT spleens continued to hypertrophy, Tie-Tg spleens shrank and became atrophic (data not shown). This was accompanied by a marked dilation of transgenic mesenteric vessels. Notably, a more detailed histological survey of vascular organs 18 hours after this LPS treatment revealed significant organ damage in transgenic, but not control, mice (Figure 2B; see also Supplemental Figure 1B). This included: loss of splenic, hepatic, and pulmonary architecture; evidence of parenchymal and endothelial apoptosis; as well as leukocyte extravasation, especially in the liver. Consistent with this, TUNEL analysis of serial sections revealed a significant increase in apoptotic cells in Tie-Tg, but not control, mice. Splenic changes were notable for a dramatic increase in red pulp, with an elevated basal apoptosis that increased significantly with LPS treatment (predominately lymphocytes in white pulp). Likewise, LPS-dependent changes in transgenic liver were associated with a significant increase in parenchymal and endothelial apoptosis (see also Figure 3A and Supplemental Figure 2A). There was also evidence of lymphocytic apoptosis. Transgenic pulmonary changes were notable for an LPS-induced alveolar septal hypertrophy, with significant lymphocytic infiltration and edema, as well as some lymphocytic apoptosis. In sum, these observations suggested that NF-κB signaling plays an important role in protecting vascular organs from damage during sepsis. Moreover, the significant increase in apoptotic endothelium in Tie-Tg mice was consistent with prior studies on isolated NF-κB–defective ECs (9, 24, 25).

*EC response to LPS- and TNF-induced stress.* To more carefully evaluate endothelial dysfunction in LPS-treated mice, hepatic vessels from Tie-Tg and littermate control mice were evaluated with immunohistochemical stains for PECAM-1 (i.e., CD31) and activated caspase-3 (Figure 3A). PECAM-1–positive endothelium was readily visualized in WT and Tie-Tg samples after 18 hours of LPS or PBS treatment. However, only LPS-treated Tie-Tg endothelium was positive for activated caspase-3, indicating onset of apoptosis. Electron microscopic (EM) analysis of these specimens provided additional evidence of LPS-induced apoptosis in Tie-Tg pulmo-
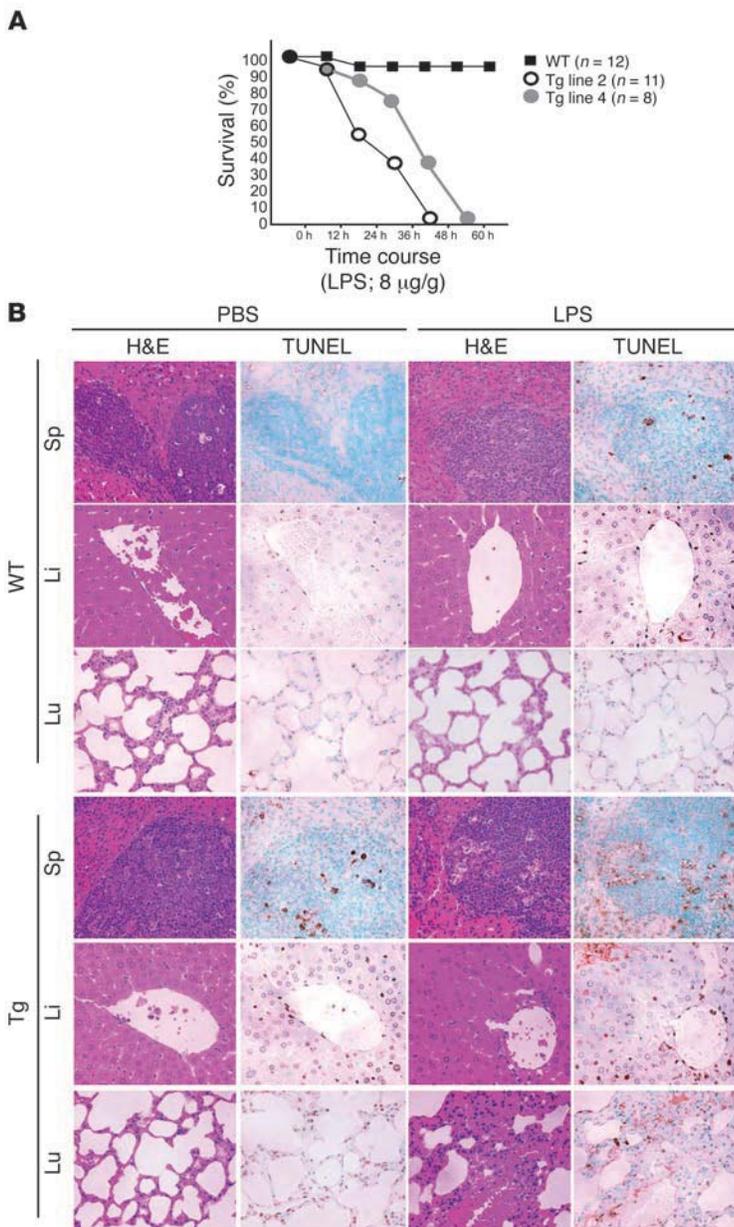
**Figure 2**
Tie-Tg mice exhibit increased sensitivity to LPS-induced toxemia. (**A**) Transgenic mice (Tie-Tg lines 2 and 4) and littermate control WT mice were injected with LPS (8 μg/g, i.v.) and evaluated for survival by a Kaplan-Meier plot. Similar results were obtained for Tie-Tg lines 1 and 3 (data not shown). (**B**) Matched H&E- and TUNEL-stained paraffin-embedded tissues (spleen, liver, and lung) from transgenic (line 2) and WT littermate control mice 18 hours after PBS or LPS (2 μg/g weight) injection, as visualized with an ×20 objective. TUNEL-positive cells are revealed by brown stain. Similar results were obtained for Tie-Tg line 4.

nary, but not control, endothelium (Supplemental Figure 2C). Consistent with this apoptotic response, by 24 hours after LPS treatment, transgenic endothelium was severely compromised, with a loss in staining for both PECAM-1 and ICAM-1 (see Supplemental Figure 2B). It was difficult to reconcile whether the loss of expression of ICAM-1, a reported NF-κB target gene, reflected extensive tissue damage and/or a blockade in NF-κB signaling.

The preceding in vivo studies suggested that Tie-Tg endothelium was prone to apoptosis. To more directly test this possibility, ECs were harvested from the lungs of transgenic and littermate control mice and cultured on collagen-coated plates. Importantly, WT and transgenic ECs did not exhibit significant differences in growth or viability during a 2-week culture period. However, transgenic ECs did demonstrate a marked reduction in the ability to translocate the p65 subunit of NF-κB to the nucleus in response to a brief stimulation with TNF-α (Figure 3B). WT ECs, in contrast, demonstrated the anticipated rapid and robust p65 nuclear translocation (24). This failure to activate p65 was also associated with a significant increase in EC apoptosis, which became apparent with more prolonged TNF-α treatment (Figure 3C). Specifically, a significant increase in pyknotic nuclei was observed in transgenic, but not control, ECs (21% versus 5%; Figure 3, C and D). These observations provide evidence that transgenic sIκBα effectively blocks NF-κB activation in ECs and that this correlates directly with an enhanced apoptotic response to TNF-α and LPS.

*Endothelial function during tumorigenesis.* In addition to its important vascular function, endothelium is increasingly recognized for its critical role in tumorigenesis (reviewed in refs. 5–7, 10). Although endothelium provides nourishment to tumors, it also serves as a barrier to metastatic cells (28). To determine whether Tie-Tg endothelial function was compromised during tumorigenesis, B16-BL6 metastatic melanoma cells were injected into transgenic mice (29, 30). After 14 days Tie-Tg lungs exhibited significantly more tumor growth than littermate control mice (i.e., WT), by both visual inspection (Figure 4A) and systematic quantification (Figure 4C; ~5-fold increase in lung weight in Tie-Tg versus controls; $P < 0.0001$). Histological analysis of size-matched metastatic lesions revealed a striking increase in tumor vascularization in transgenic mice (Figure 4B; see also Figure 5B).

Even though B16-BL6 tumors are considered to be resistant to host immunity (29), the expression of sIκBα in immune tissues (see Figure 1, B and C) raised the possibility that a defective immune response in Tie-Tg mice could contribute to their enhanced metastatic phenotype. Consistent with reports that the Tie2 enhancer/promoter can direct expression of transgenes in hematopoietic cells (31, 32), Tie-Tg lymphocytes exhibited defective NF-κB activation (data not shown). As in previous studies in which sIκBα expression had been specifically targeted to lymphocytes, Tie-Tg T cells were impaired in their ability to proliferate and secrete IL-2 in response to stimulation with anti-CD3 and anti-CD28 (data not shown; refs. 15, 16, 33).

To exclude the possibility that a defective immune response contributed to the enhanced tumorigenesis in Tie-Tg mice, 2 additional studies were undertaken. The first study compared tumorigenesis in Tie-Tg and immunodeficient Rag2$^{-/-}$ mice. Tumor burden was found to be considerably higher in Tie-Tg than Rag$^{-/-}$ mice (15.6% versus 3%, $P < 0.005$; 1% for WT mice; Supplemental Figure 3B), suggesting that immune defects are unlikely to account for the Tie-Tg tumor phenotype.
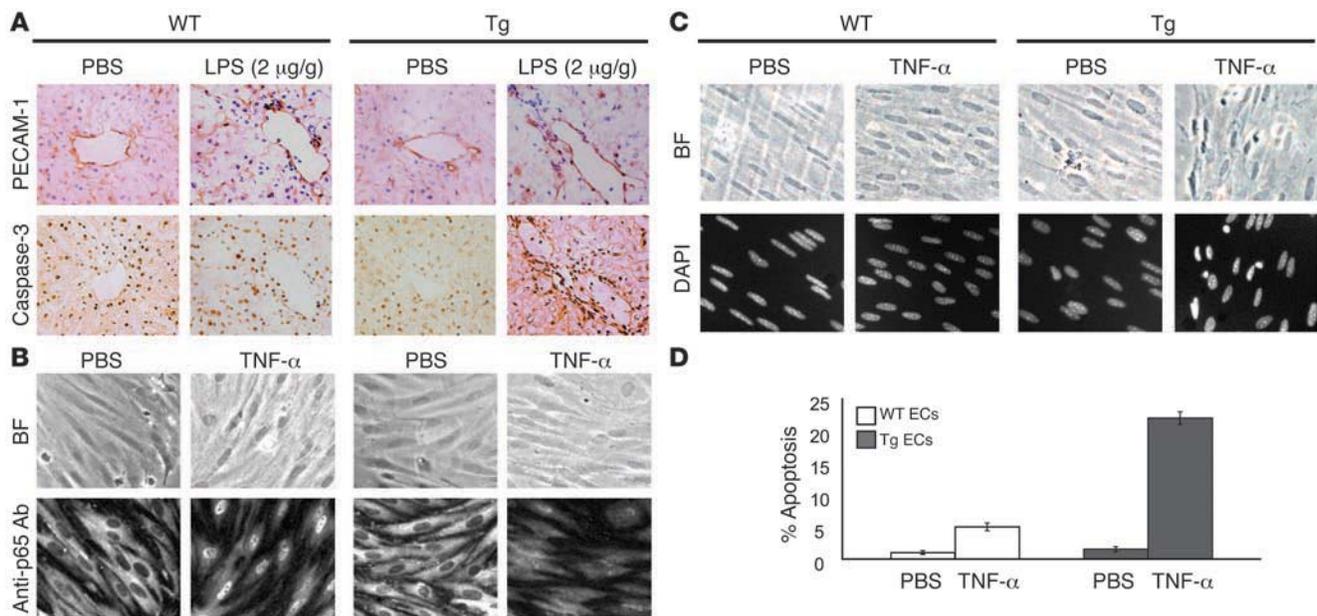
**Figure 3**
Transgenic ECs exhibit enhanced apoptosis. (**A**) Frozen hepatic tissue sections prepared from WT and Tie-Tg (line 2) mice 18 hours after PBS or LPS (2 μg/g weight) injection, stained for PECAM-1 and caspase-3 (anti–active caspase-3–specific antibody) and then visualized under a ×20 objective. Similar results were obtained with Tie–Tg line 4. (**B**) Immunostaining revealed a defect in the nuclear translocation of p65 in TNF-α–stimulated (100 ng/ml, 1 hour) cultured primary, pulmonary transgenic ECs. Phase-contrast bright-field (BF) images (×100 objective) of the same cells are shown in the upper panels. ECs were prepared from WT and Tie-Tg lines 2 and 4. (**C**) Cultured primary transgenic ECs exhibit enhanced nuclear fragmentation after TNF-α (100 ng/ml, 4.5 hours) stimulation, as revealed by DAPI staining (lower panels). Phase-contrast bright-field images (×100 objective) of the same cells are shown in the upper panels. (**D**) Quantification of the nuclear fragmentation/apoptosis data presented in **C**. Analysis represents the percentage of cells exhibiting clear nuclear fragmentation in 5 independent fields of 100 cells. Evaluation was performed by a researcher blinded to the experimental protocol.

A second, more rigorous study employed BM transplantation (BMT) to directly evaluate the contribution of endothelial sIκBα expression to the enhanced proclivity for tumor growth. Reciprocal BMTs were carried out. Homotypic transplants served as controls (i.e., WT→WT and Tg→Tg). In addition, to facilitate evaluation of engraftment efficiency, WT BM transplanted into Tie-Tg mice was harvested from β-actin–GFP+ mice (i.e., β-actin→Tg). Littermate WT control mice were transplanted with BM from Tie-Tg mice (Tg→WT). After 2 months, effective engraftment was confirmed either through FACS analysis of circulating leukocytes (i.e., ≥95% reconstitution for β-actin→Tg mice) or with a transgene-specific PCR (see Supplemental Figure 3A). Transplanted mice were then injected with B16-BL6 melanoma cells, as before, and evaluated for pulmonary tumor burden 14 days later (Figure 5A). Transgenic mice transplanted with WT β-actin–GFP+ BM (β-actin→Tg; n = 6) or transgenic (self; Tg→Tg; n = 3), developed substantially more metastatic disease (i.e., 23% and 31%) than the appropriately matched WT control mice. Specifically, tumor burden was approximately 5% in each of the 3 control groups, WT (n = 3), Tg→WT (n = 6), and WT→WT (n = 3), demonstrating that transgenic hematopoietic cells do not significantly contribute to the enhanced tumor phenotype of transgenic mice. Finally, Tie-Tg mice engrafted with WT BM (β-actin→Tg) developed a tumor burden similar to Tie-Tg (or Tg→Tg) mice, indicating that the "pro-tumor" phenotype can be directly attributed to a functional defect in transgenic endothelium.

The enhanced tumor growth in transgenic mice was associated with a marked increase in tumor vasculature, suggesting that the proclivity of Tie-Tg endothelium for acute apoptosis, seen with LPS treatment (Figure 2B, Figure 3, and Supplemental Figure 2), was unlikely to account for the enhanced transgenic tumor burden (Figure 5B). Rather, transgenic tumors demonstrated a significant increase in the staining for 3 EC markers (PECAM-1, CD34, and ICAM-1; Figure 5B), more consistent with an increased angiogenic potential. Even more striking was the disorganized nature of this robust transgenic tumor vasculature, raising the possibility that NF-κB–dependent signals may normally serve to regulate the ordered process of angiogenesis.

To test the angiogenic potential of transgenic endothelium, B16-BL6–impregnated Matrigel was injected into Tie-Tg and littermate control mice and recovered 5 days later. Staining for PECAM-1 revealed a striking increase in number of vessel that penetrated the Matrigel plugs from Tie-Tg mice (n = 4; Figure 5C). In contrast, Matrigel plugs from control mice (n = 4) exhibited only modest peripheral vascular penetration. Moreover, transgenic vessels were fully formed, illustrating a robust angiogenic potential.

*Transgenic endothelium demonstrates increased permeability.* Next, we considered whether enhanced vascular permeability evident in pulmonary parenchyma after LPS treatment might also account for the enhanced tumor metastasis and growth observed in the Tie-Tg mice. First, the vascular permeability was directly evaluated through a challenge with topical mustard oil, an effective inflammatory stimulant. Transgenic tissue exhibited an approximately 4.5-fold increase in Evans blue dye extravasation after application of mustard oil, indicating enhanced vascular leakiness (see Figure 6A;
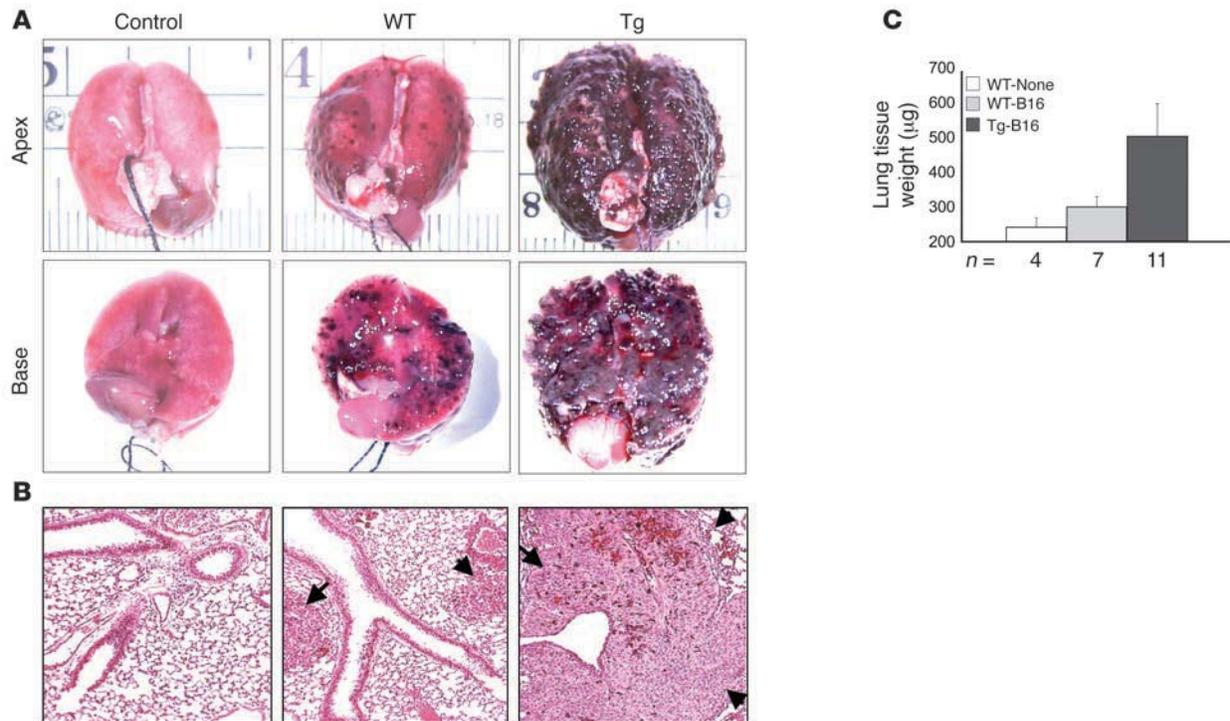
**Figure 4**
Tie-Tg mice exhibit enhanced B16-BL6 metastatic lung disease. (**A**) Gross evaluation of lungs reveals that Tie-Tg mice develop substantially more and larger metastases 14 days after B16-BL6 melanoma injection ($5 \times 10^5$ cells, i.v.). Images are representative of results obtained from WT and Tie-Tg (lines 2 and 4) mice. (**B**) H&E analysis with a ×10 objective of sections obtained from the lungs shown in **A**. Metastases are marked with arrows. (**C**) Metastasis was quantified by change in lung weight compared with a nonexposed control. Lung mass was determined in WT or Tg mice, either before (None) or after B16-BL6 tumorigenesis (B16; as in **A**). Total lung mass increased an average of 50 μg in WT and 250 μg in Tie-Tg lungs ($P < 0.0001$) compared with nonexposed controls. Data represent mice from both transgenic lines.

$P < 0.009$). Second, ultrastructural studies were undertaken to determine whether intrinsic differences in the TJs between transgenic and control ECs might account for vascular leakiness and the enhanced metastatic potential in transgenic mice. For these studies, samples were prepared from WT and transgenic lungs, before and after a challenge with LPS or B16-BL6 tumor. EM analysis of untreated mice revealed that TJs were notably less dense in transgenic mice, with an approximately 2-fold increase in diameter (i.e., distance between cells; Figure 6B; refs. 34–37). Although transgenic TJs exhibited a similar, approximately 2-fold increase in diameter in LPS-challenged mice, fewer were observed per ×3,320 power EM field. This could at least in part be attributed to an increase in transgenic endothelial apoptosis (see Supplemental Figure 2C). The most dramatic differences were evident in the pulmonary vasculature of B16-BL6–challenged mice. In WT mice, tumor-proximal endothelial TJs were found at the expected frequency (~2.5 TJs per ×3,320 power EM field; 8 fields observed) but exhibited an approximately 2-fold increase in diameter compared with untreated controls. In contrast, no intact TJs were observed in eight ×3,320 EM fields in Tie-Tg tumor-proximal vessels. Rather, only fragmented TJs with small diameters were found (Figure 6B), indicating a significant loss of structural integrity.

In summary, these studies demonstrate that the enhanced metastatic tumor burden in sIκBα transgenic mice correlates directly with an increase in vascular permeability, associated with a defective TJ structure.

## Discussion
Vascular endothelium maintains a vital, dynamic interface between cells of the circulatory system and the tissues they perfuse. In addition to facilitating the diffusion of nutrients, it also plays important roles in regulating circulatory homeostasis and leukocyte trafficking. More recently, the endothelium has been ascribed an important role in tumorigenesis (5). Thus, there is great interest in identifying factors, as well as their downstream signaling components, that regulate endothelial activity in health and disease (reviewed in refs. 1, 5–7, 10).

Although NF-κB and activating receptors were first described in immune cells, they are now recognized as playing a pervasive role in directing host response to environmental stress (12, 17). For example, NF-κB activity has been associated with the expression of inflammatory mediators and the regulation of programmed cell death in endothelium, albeit largely in cultured ECs (3, 4, 8, 9, 25, 34–37). An effort to extend these studies to a more physiological setting has in part been thwarted by phenotypic limitations of NF-κB–knockout mice (12, 19). As an alternative approach, the Tie-2 promoter/enhancer was exploited to direct the expression of a dominant interfering NF-κB mutant, sIκBα, to the endothelium and some leukocytes as well (21, 31, 38). Although none of the 4 transgenic lines that were generated exhibited developmental defects, their response to challenge with LPS and cancer was quite abnormal, underscoring the important role NF-κB plays in regulating endothelial activity.
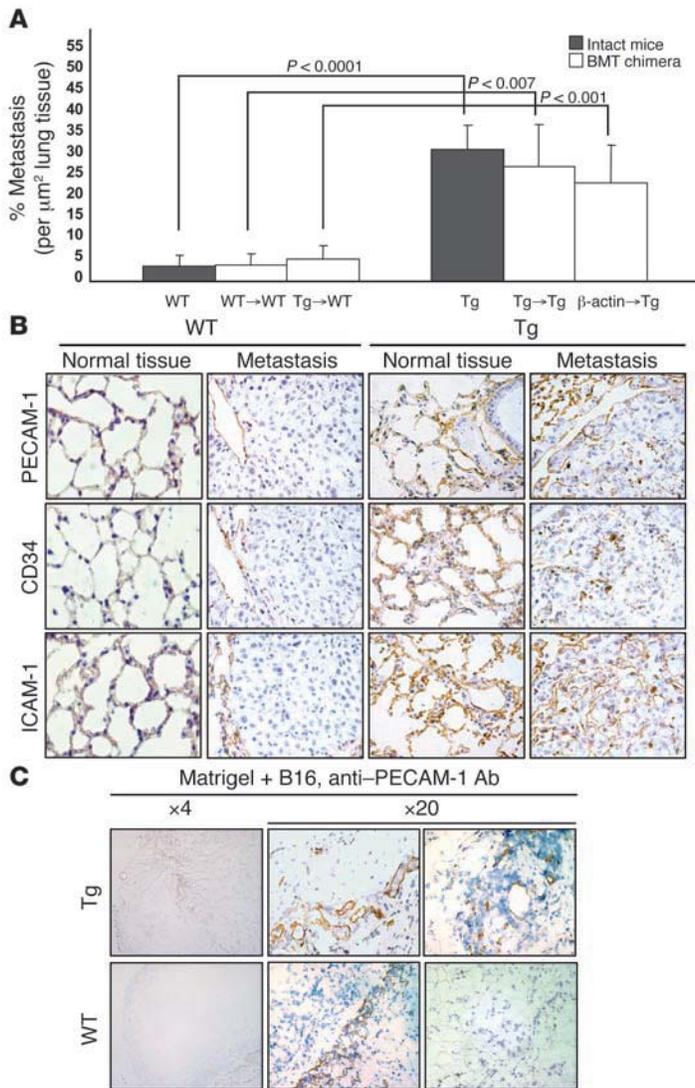
**Figure 5**
Enhanced tumorigenesis in Tie-Tg mice is endothelial cell intrinsic. (**A**) WT and transgenic mice were engrafted with either transgenic or WT (from β-actin–GFP+ mice) BM. Quantification of tumor mass (percent metastasis per micrometer squared of lung tissue) demonstrated that mice with transgenic ECs (i.e., Tg, $n = 4$; Tg→Tg, $n = 3$; and β-actin→Tg, $n = 6$) exhibited considerably higher tumor burdens (respectively, 31%, 27%, and 23% versus 3.6%, 3.9%, and 5.2%; $P < 0.0001$, $P < 0.007$, and $P < 0.001$) than mice with WT ECs (i.e., WT, $n = 3$; WT→WT, $n = 3$; and Tg→WT, $n = 6$). Five fields were evaluated per mouse. Data represent mice from transgenic lines 2 and 4. (**B**) A significant increase in tumor vascularization in mice with transgenic ECs was revealed by PECAM-1 (CD31), CD34, and ICAM-1 immunostaining visualized under a ×20 objective. (**C**) Neovascularization in B16-BL6 cell–impregnated Matrigel was significantly increased when transplanted into Tg mice. Blood vessels were revealed by staining for PECAM-1 and visualized under ×4 and ×20 objectives, as indicated.

When challenged with LPS, each of the 4 Tie-Tg lines developed multiorgan failure that was associated with increased endothelial apoptosis. Curiously, transgene-dependent blockade of NF-κB signaling was less extensive in transgenic ECs than in the corresponding transgenic T cells (data not shown). This observation, along with evidence of endothelial structural

defects (see below), raised the intriguing possibility that a more complete blockade of endothelial NF-κB was selected against, because it led to a developmentally lethal phenotype (12). This model also accounts for our relatively low yield of transgenic founders.

One important defect in Tie-Tg endothelium was the marked increase in vascular permeability observed in mice treated with LPS (especially in lungs; Figure 2B) or mustard oil (Figure 6A). To explore the potential consequence of this compromised barrier activity, transgenic mice were subsequently challenged with B16-BL6 melanoma cells, a model for metastatic cancer. Consistent with a barrier defect, transgenic mice exhibited a substantial increase in number of metastatic lesions (Figure 4). Intriguingly, this was not associated with endothelial apoptosis, as was the case with LPS treatment but rather a striking increase in tumor vascular density (Figure 5). Matrigel studies provided additional evidence for enhanced angiogenic potential of Tie-Tg endothelium. Of note, transgenic tumor vasculature was disorganized, an observation that has recently been ascribed to defective interactions between pericytes and ECs (7). Thus, endothelial NF-κB activity (e.g., perhaps in response to trophic pericyte stimulation) may normally serve to promote the formation of an organized vasculature (i.e., with healthy TJs; see below). The absence of this organizing activity may free endothelium for a more robust angiogenic response.

Two additional sets of studies were carried out in the B16-BL6 tumor model. The first set employed BMT to exclude the possibility that defective immunosurveillance, caused by transgene expression in lymphocytes (data not shown), might contribute to the enhanced tumor phenotype (Figure 5). The second approach exploited EM, which documented significant changes in the structural integrity of transgenic, tumor-proximal endothelial TJs. Intriguingly, increased metastatic potential of human melanomas has recently been correlated with a decreased expression of claudin-1, a component of the TJ, in tumor-associated vessels (39). Therefore, a set of immunohistochemical studies was carried out to determine whether analogous changes might account for decreased TJ density observed in transgenic endothelium. However, no differences in staining for zona occludens 1 (ZO-1) or claudin-1 were observed (data not shown), supporting other evidence that increased vascular permeability is often associated with changes in the distribution, association, and/or activity of TJ proteins, rather than changes in their absolute level of expression (40–43). Although our studies demonstrate that NF-κB participates in the regulation of endothelial barrier activity, they did not exclude an additional role for NF-κB in regulating the expression of adhesion molecules, which have recently been shown to direct endothelial progenitor cell recruitment in response to tumor-derived growth factor(s) (28). Future studies will explore the complex but likely dynamic relationship among TJ integrity, barrier activity, and enhanced angiogenesis.

Evidence that transgenic endothelium exhibited both an increased sensitivity to LPS-induced apoptosis and promoted enhanced tumor angiogenesis, raised the intriguing possibility that LPS injection might reduce tumor burden. Unfortunately, the overall heightened sensitivity of transgenic mice to LPS prevented a meaningful evaluation of this idea, as the mice rapidly
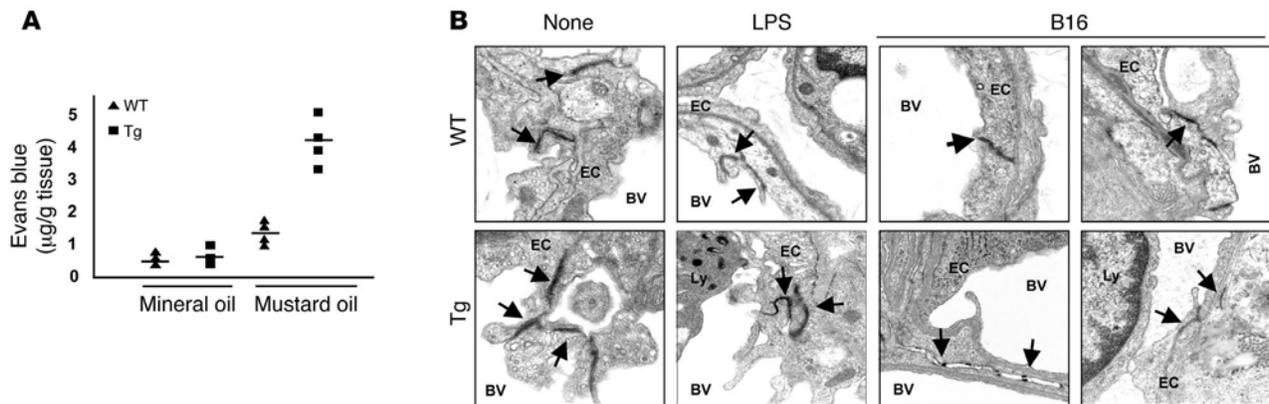
## Figure 6

Enhanced EC leakiness in the transgenic mice. (**A**) Vascular permeability in transgenic (line 4; *n* = 4) and the WT mice (*n* = 4) was measured in response to mustard oil with Evans blue dye. Local vascular permeability was increased 4.5-fold in transgenic (*P* < 0.009) and 2-fold in WT mice (*P* < 0.0001). No difference was observed in unstimulated mice (*n* = 4 for each genotype). Similar results were obtained with Tie-Tg line 2. (**B**) TJs of pulmonary endothelium were evaluated by EM. Lung tissue was harvested from WT or transgenic mice either before (None) or after LPS (2 μg/ml, 18 hours) treatment or 14 days after B16-BL6 tumor injection. Specimens prepared for EM were initially screened at a magnification of ×3,320 (see Supplemental Figure 3C). Areas with adjoining ECs (as indicated in Supplemental Figure 3C) were then examined at a magnification of ×9,960 and are presented in 8 panels, as indicated. Electron-dense TJs are marked with arrows. Other features are marked as EC (endothelial cells), Ly (white blood cells), BV (blood vessels), and B16 (B16–BL6 melanoma cells). EMs are representative images from 3–8 random ×3,320 fields per sample and represent tissues from Tie-Tg lines 2 and 4.

became moribund. However, tumor vasculature in LPS-treated Tie-Tg mice did exhibit a hypertrophied endothelium, suggestive of pending apoptosis.

Our studies underscore the important role NF-κB plays in regulating endothelial response(s) to both acute and nonacute stresses, which includes regulating barrier activity, angiogenic potential, and protection from apoptosis. Moreover, all 3 of these phenotypic responses may be associated with the altered TJ structure in transgenic mice. For example, early (i.e., 18 hours) after LPS treatment, transgenic mice exhibited an acute reduction in barrier activity that was associated with both decreased TJ density (Figure 6B; refs. 44, 45) and increased apoptosis (due to a loss in NF-κB's prosurvival activity) (Figure 2B and Figure 3; refs. 9, 18, 25, 43). Of note, the relative number of apoptotic ECs increased steadily over time (e.g., Supplemental Figure 2B). Intriguingly, studies in LPS-treated bovine ECs have indicated that proapoptotic caspases rapidly cleave TJ component proteins (45). Thus, caspases, whose activity is antagonized by NF-κB (see Figure 3A; refs. 12, 17, 46, 47), may be responsible both for decreased barrier function and increased apoptosis. In contrast, the nonacute changes associated with enhanced tumorigenesis in transgenic mice appears to reflect both basal changes in TJ structure (i.e., decreased barrier activity) and a more gradual, yet dramatic compromise of TJ structure that is associated with tumor growth (e.g., angiogenesis).

Evidence for an extensive role in regulating endothelial activity raises a cautionary note about pharmaceutical agents that are being developed to target NF-κB activity.

## Methods

*Transgene construction and generation of transgenic mice.* To direct the expression of sIκBα (S32A/S36A; ref. 14) in ECs, the cDNA was cloned into a transgenic vector provided by T. Sato (Weill Medical College of Cornell University, New York, New York, USA) (consisting of a 2-kb Tie2 promoter, 1.7-kb human growth hormone (hGH) polyadenylation cassette, and the 10-kb Tie2 enhancer; Figure 1A; ref. 21). This entailed introduction of a FLAG tag at the amino terminus of sIκBα (by PCR-based mutagenesis; Stratagene) and cloning into ClaI and XbaI endonuclease restriction sites between the Tie2 promoter and hGH polyadenylation cassette (see Figure 1A). The transgenic construct was linearized with SalI and microinjected into fertilized C57BL/6J × CBA F$_1$ hybrid eggs, which were implanted in pseudopregnant Swiss Webster foster mothers at the Columbia University Transgenic Facility. F$_1$ offspring were genotyped by Southern blotting *Hind*III-digested tail DNA with a [$^{32}$P]dCTP-labeled IκBα probe. The transgene copy number was determined through PhosphorImager (Molecular Dynamics Inc.) analysis. All animal studies were carried out by protocols approved by the Columbia University Institutional Animal Care and Use Committee (AC-AAAA0704, AAAA2565, AAAA4096).

*Cell culture.* HEK 293T cells (ATTC), B16-BL6 melanoma cells (gift of A. Diefenbach, New York University, New York, New York, USA; ref. 48) were cultured at 37°C, 5% CO$_2$ in DMEM supplemented with 10% heat-inactivated FCS, 100 U/ml penicillin/streptomycin, 2 mM glutamine. ECs were isolated from murine lungs as previously described (49). Briefly, tissue from 5 lungs was homogenized and treated with collagenase A (330 U/ml; Sigma-Aldrich) and DNase I (150 U/ml; Sigma-Aldrich) at 37°C for 30 minutes. Single-cell suspensions, in PBS plus 1% BSA, were incubated with anti-CD31 mAb (2 μg/ml rat anti-mouse, 1 hour; BD Biosciences — Pharmingen). ECs were purified by subsequent incubation with M-450 Dynabeads (1 hour at 4°C; 25 μl beads; Dynal) coupled with sheep anti-rat IgG, as per the manufacturer's instructions. Isolated ECs were cultured in EGM-2 media (Cambrex) at 37°C, 8% CO$_2$ on collagen-coated plates (Cell Prime 100, 1:30; Cohesion Inc.). Thymic and splenic lymphocytes were cultured in RPMI supplemented with 10% FCS (heat inactivated; HyClone), 100 U/ml penicillin/streptomycin (Invitrogen), 2 mM glutamine (Invitrogen), with or without IL-2 (20 U/ml; Roche Diagnostics). Splenic CD4$^+$ T lymphocytes were isolated with anti-CD4–coupled Macs beads (Miltenyi Biotec), as per the vendor's directions.

*RT-PCR.* Total RNA was isolated from murine tissues by TRIZOL reagent (Invitrogen). cDNA was prepared with AMV reverse transcriptase from 2 μg of total oligo-(dT)$_{15}$–primed RNA (Promega) and amplified with specific

primers (FLAG-Tag, 5′-CCATGGACTACAAAGACGATGACG-3′; IκBα forward, 5′-AGACCTGGCTTTCCTCAACTTCC-3′; IκBα reverse, 5′-CAGCACCCAAGGACACCAAAAGC-3′; hGH forward, 5′-AGCCACT-GCCGGTCC-3′; hGH reverse, 5′-GGCCAAGCGCTTGGGCACT-GTTCCCTCCCT-3′; and GAPDH (50).

*Histopathology.* Tissue samples were fixed in 10% formalin (24 hours), embedded in paraffin, sectioned (5 μm), and stained with H&E to analyze tissue morphology. Alternatively, samples were embedded in OCT (Tissue-Tek; Sakura), snap-frozen, sectioned (5 μm), and fixed (cold acetone, 5 minutes). These samples were blocked with 30% $H_2O_2$ (for endogenous peroxidase), Avidin/Biotin Blocking Kit (Vector Laboratories), and goat serum, prior to staining with anti-CD31/PECAM-1 (1:500; BD Biosciences — Pharmingen), ICAM-1 (1:100; Abcam), CD34 (1:100; BD Biosciences), anti–caspase-3 (active isoform; 1:500; R&D Systems), ZO-1 (1:250; BD Biosciences), and claudin-1 (1:100; Abcam). Bound antibodies were revealed with a biotinylated secondary antibody (goat anti-rabbit; 1:500; BD Biosciences) and a DAB Substrate Kit (Vector Laboratories; refs. 51, 52). Apoptosis in paraffin-embedded sections was revealed by TUNEL staining (53) as per the manufacture's directions (kit S7101; Chemicon International).

p65 nuclear translocation in ECs or thymocytes stimulated with TNF-α (100 ng/ml; R&D Systems) was evaluated as previously reported (54). Briefly, fresh thymocytes, spun onto anti-CD3–coated plates, or cultured ECs, were fixed with 10% formaldehyde (20 minutes; Fisher Scientific), permeabilized (1% Triton-X 100; Sigma-Aldrich), and blocked with 3% BSA in Tris-buffered saline with Tween-20 (Sigma-Aldrich). Samples were stained with anti-p65 (1:1,000; 1 hour at room temperature; Santa Cruz Biotechnology Inc.) and Cy3-conjugated secondary antibody (donkey anti-rabbit; 1:500 for 30 minutes at room temperature; Rockland). Samples were also counterstained with DAPI (Sigma-Aldrich) to visualize nuclei. Slides were analyzed by Nikon Eclipse TE-300 florescence microscopy, as previously reported (54).

For EM, untreated, LPS-treated, or B16-BL6–treated mice were anesthetized and fixed by vascular perfusion with 2.5% glutaraldehyde in 0.1 M Sorenson's buffer (pH 7.2) for 10 minutes, postfixed with 1% $OsO_4$ in 0.1 M Sorenson's buffer, and embedded in Lx-112 (Ladd Research Industries). Thin sections (60 nm) were cut on an RMC MT-7000 microtome, stained with toluidine blue, and examined by transmission EM on a JEOL JEM-1200 EXII equipped with a digital camera at ×3,320 and ×9,960, as previously reported (55).

*Western blot analysis.* Protein extracts were prepared by cellular lysis in a 0.5% NP-40–based buffer as previously reported (54). Extracts were fractionated by SDS-PAGE directly or after immunoprecipitation (anti-IκBα; 3 μg/precipitation; 16 hours at 4°C) and immunoblotted as previously reported (54). Filters were probed with anti-FLAG (M5; 1:1,000; 1 hour at room temperature; Sigma-Aldrich) and detected by ECL (Amersham Biosciences).

*Flow cytometry.* PBLs (tail vein) were treated with red cell lysis buffer (Sigma-Aldrich) and evaluated for side scatter (SSC) and GFP-dependent fluorescence. Apoptosis was evaluated with annexin V and propidium iodide staining (BD Biosciences — Pharmingen). Samples were analyzed on a FACSCaliber (BD). Each plot represents analysis of more than $10^4$ events.

*Evans blue vascular permeability assay.* Mustard oil (5% allyl-isothiocyanate in mineral oil; Sigma-Aldrich) was applied twice ($t$ = 15 minutes) to the dorsal and ventral surfaces of the right ear of mice following the i.v. injection of Evans blue dye (30 mg/kg; Sigma-Aldrich), as previously reported (56). The left ear treated with mineral oil alone served as a control. Thirty minutes later, mice were anesthetized, and the vasculature was fixed by perfusion with 1% paraformaldehyde in 50 mM citrate buffer/pH 3.5 (1 minute at 120 mmHg). Ears were harvested, dried (6 hours, 55°C), and weighed, and Evans blue dye was extracted in 1 ml formamide (5 days, room temperature). Yield of dye was measured spectrophotometrically (λ = 610 nm) and compared with a standard curve to determine nanograms of Evans blue dye per milligram of tissue (56). Statistical analysis was carried out using unpaired 2-tailed Student's $t$ test. $P$ values less than 0.05 were considered significant.

*In vivo tumorigenesis.* Theses studies exploited the established B16-BL6 model of metastatic tumor growth (29, 30). Briefly, 300 μl of either $1 \times 10^5$ or $5 \times 10^5$ freshly harvested and washed B16-BL6 cells (PBS) were i.v. injected into study mice. After 14 days, mice were sacrificed, and the lungs were removed and weighed. Lungs were inflated, then fixed for histological evaluation.

*Matrigel assay.* Angiogenesis was assessed in Matrigel plugs (57). Transgenic ($n$ = 4) and WT ($n$ = 4) mice were inoculated with 0.1 ml of Matrigel (BD Biosciences) embedded with $1 \times 10^6$ B16-BL6 melanoma cells. Matrigel was injected subcutaneously to the ventrolateral hind flank. After 5 days Matrigel plugs were removed, fixed with 4% PFA, and embedded in 30% sucrose, snap-frozen in OCT, sectioned (5 μm), and stained for PECAM-1, as described above (58).

*BMT.* Adoptive transfers were performed as previously described (59, 60). Briefly, BM cells were sterilely harvested from the tibias and femurs of 5 β-actin–GFP$^+$ (61), C57BL/6J, or Tie-Tg mice in HBSS (Invitrogen) and filtered through a 40-μm nylon mesh (BD Biosciences — Falcon). $5 \times 10^5$ of these unfractionated cells (in 300 μl) were i.v. injected 3 hours after lethal irradiation (12 Gy). Eight weeks after transplantation, peripheral blood was evaluated for engraftment by FACS or PCR.

Address correspondence to: Christian Schindler, Columbia University, HHSC 1208, 701 West 168th Street, New York, New York 10032, USA. Phone: (212) 305-5380; Fax: (212) 543-0063; E-mail: cws4@columbia.edu.

1. Galley, H.F., and Webster, N.R. 2004. Physiology of the endothelium. *Br. J. Anaesth.* **93**:105–113.
2. Zhang, W.J., and Frei, B. 2001. Alpha-lipoic acid inhibits TNF-alpha-induced NF-kappaB activation and adhesion molecule expression in human aortic endothelial cells. *FASEB J.* **15**:2423–2432.
3. Aoki, M., et al. 2001. Endothelial apoptosis induced by oxidative stress through activation of NF-kappaB: antiapoptotic effect of antioxidant agents on endothelial cells. *Hypertension.* **38**:48–55.
4. Badrichani, A.Z., et al. 1999. Bcl-2 and Bcl-XL serve an anti-inflammatory function in endothelial cells through inhibition of NF-κB. *J. Clin. Invest.* **103**:543–553.
5. Folkman, J. 2003. Fundamental concepts of the angiogenic process. *Curr. Mol. Med.* **3**:643–651.
6. Tammela, T., Enholm, B., Alitalo, K., and Paavonen, K. 2005. The biology of vascular endothelial growth factors. *Cardiovasc. Res.* **65**:550–563.
7. Armulik, A., Abramsson, A., and Betsholtz, C. 2005. Endothelial/pericyte interactions. *Circ. Res.* **97**:512–523.
8. Lush, C.W., Cepinskas, G., and Kvietys, P.R. 2000. LPS tolerance in human endothelial cells: reduced PMN adhesion, E-selectin expression, and NF-kappaB mobilization. *Am. J. Physiol. Heart Circ. Physiol.* **278**:H853–H861.
9. Stehlik, C., et al. 1998. Nuclear factor (NF)-kappaB-regulated X-chromosome-linked iap gene expression protects endothelial cells from tumor necrosis factor alpha-induced apoptosis. *J. Exp. Med.* **188**:211–216.
10. Neri, D., and Bicknell, R. 2005. Tumour vascular targeting. *Nat. Rev. Cancer.* **5**:436–446.
11. Bonizzi, G., Piette, J., Merville, M.P., and Bours, V. 2000. Cell type-specific role for reactive oxygen spe-

cies in nuclear factor-kappaB activation by interleukin-1. *Biochem. Pharmacol.* **59**:7–11.

12. Hayden, M.S., and Ghosh, S. 2004. Signaling to NF-kappaB. *Genes Dev.* **18**:2195–2224.

13. Zheng, Y., et al. 2001. NF-kappa B RelA (p65) is essential for TNF-alpha-induced fas expression but dispensable for both TCR-induced expression and activation-induced cell death. *J. Immunol.* **166**:4949–4957.

14. Wang, C.Y., Mayo, M.W., and Baldwin, A.S., Jr. 1996. TNF- and cancer therapy-induced apoptosis: potentiation by inhibition of NF-kappaB. *Science.* **274**:784–787.

15. Esslinger, C.W., Wilson, A., Sordat, B., Beermann, F., and Jongeneel, C.V. 1997. Abnormal T lymphocyte development induced by targeted overexpression of IkappaB alpha. *J. Immunol.* **158**:5075–5078.

16. Hettmann, T., DiDonato, J., Karin, M., and Leiden, J.M. 1999. An essential role for nuclear factor kappaB in promoting double positive thymocyte apoptosis. *J. Exp. Med.* **189**:145–158.

17. Luo, J.L., Kamata, H., and Karin, M. 2005. IKK/NF-κB signaling: balancing life and death — a new approach to cancer therapy. *J. Clin. Invest.* **115**:2625–2632. doi:10.1172/JCI26322.

18. Papa, S., Zazzeroni, F., Pham, C.G., Bubici, C., and Franzoso, G. 2004. Linking JNK signaling to NF-kappaB: a key to survival. *J. Cell Sci.* **117**:5197–5208.

19. Zheng, Y., Vig, M., Lyons, J., Van Parijs, L., and Beg, A.A. 2003. Combined deficiency of p50 and cRel in CD4+ T cells reveals an essential requirement for nuclear factor kappaB in regulating mature T cell survival and in vivo function. *J. Exp. Med.* **197**:861–874.

20. Prendes, M., Zheng, Y., and Beg, A.A. 2003. Regulation of developing B cell survival by RelA-containing NF-kappa B complexes. *J. Immunol.* **171**:3963–3969.

21. Schlaeger, T.M., et al. 1997. Uniform vascular-endothelial-cell-specific gene expression in both embryonic and adult transgenic mice. *Proc. Natl. Acad. Sci. U. S. A.* **94**:3058–3063.

22. Kisanuki, Y.Y., et al. 2001. Tie2-Cre transgenic mice: a new model for endothelial cell-lineage analysis in vivo. *Dev. Biol.* **230**:230–242.

23. Arai, F., et al. 2004. Tie2/angiopoietin-1 signaling regulates hematopoietic stem cell quiescence in the bone marrow niche. *Cell.* **118**:149–161.

24. Brouard, S., et al. 2002. Heme oxygenase-1-derived carbon monoxide requires the activation of transcription factor NF-kappa B to protect endothelial cells from tumor necrosis factor-alpha-mediated apoptosis. *J. Biol. Chem.* **277**:17950–17961.

25. Cooper, J.T., et al. 1996. A20 blocks endothelial cell activation through a NF-kappaB-dependent mechanism. *J. Biol. Chem.* **271**:18068–18073.

26. Bannerman, D.D., and Goldblum, S.E. 2003. Mechanisms of bacterial lipopolysaccharide-induced endothelial apoptosis. *Am. J. Physiol. Lung Cell. Mol. Physiol.* **284**:L899–L914.

27. Grandel, U., and Grimminger, F. 2003. Endothelial responses to bacterial toxins in sepsis. *Crit. Rev. Immunol.* **23**:267–299.

28. Kaplan, R.N., et al. 2005. VEGFR1-positive haematopoietic bone marrow progenitors initiate the premetastatic niche. *Nature.* **438**:820–827.

29. Arca, M.J., Krauss, J.C., Strome, S.E., Cameron, M.J., and Chang, A.E. 1996. Diverse manifestations of tumorigenicity and immunogenicity displayed by the poorly immunogenic B16-BL6 melanoma transduced with cytokine genes. *Cancer Immunol. Immunother.* **42**:237–245.

30. Nakamura, K., et al. 2002. Characterization of mouse melanoma cell lines by their mortal malignancy using an experimental metastatic model. *Life Sci.* **70**:791–798.

31. Koni, P.A., et al. 2001. Conditional vascular cell adhesion molecule 1 deletion in mice: impaired lymphocyte migration to bone marrow. *J. Exp. Med.* **193**:741–754.

32. Constien, R., et al. 2001. Characterization of a novel EGFP reporter mouse to monitor Cre recombination as demonstrated by a Tie2 Cre mouse line. *Genesis.* **30**:36–44.

33. Boothby, M.R., Mora, A.L., Scherer, D.C., Brockman, J.A., and Ballard, D.W. 1997. Perturbation of the T lymphocyte lineage in transgenic mice expressing a constitutive repressor of nuclear factor (NF)-kappaB. *J. Exp. Med.* **185**:1897–1907.

34. Soler, A.P., et al. 1999. Activation of NF-kappaB is necessary for the restoration of the barrier function of an epithelium undergoing TNF-alpha-induced apoptosis. *Eur. J. Cell Biol.* **78**:56–66.

35. Ma, T.Y., et al. 2004. TNF-alpha-induced increase in intestinal epithelial tight junction permeability requires NF-kappa B activation. *Am. J. Physiol. Gastrointest. Liver Physiol.* **286**:G367–G376.

36. Andras, I.E., et al. 2005. Signaling mechanisms of HIV-1 Tat-induced alterations of claudin-5 expression in brain endothelial cells. *J. Cereb. Blood Flow Metab.* **25**:1159–1170.

37. Brown, R.C., et al. 2003. Protection against hypoxia-induced increase in blood-brain barrier permeability: role of tight junction proteins and NFkappaB. *J. Cell Sci.* **116**:693–700.

38. Laouar, Y., Welte, T., Fu, X.Y., and Flavell, R.A. 2003. STAT3 is required for Flt3L-dependent dendritic cell differentiation. *Immunity.* **19**:903–912.

39. Cohn, M.L., et al. 2005. Loss of claudin-1 expression in tumor-associated vessels correlates with acquisition of metastatic phenotype in melanocytic neoplasms. *J. Cutan. Pathol.* **32**:533–536.

40. Lee, H.S., et al. 2004. Hydrogen peroxide-induced alterations of tight junction proteins in bovine brain microvascular endothelial cells. *Microvasc. Res.* **68**:231–238.

41. Martin, T.A., Das, T., Mansel, R.E., and Jiang, W.G. 2006. Synergistic regulation of endothelial tight junctions by antioxidant (Se) and polyunsaturated lipid (GLA) via Claudin-5 modulation. *J. Cell. Biochem.* **98**:1308–1319.

42. Soma, T., et al. 2004. Thr(207) of claudin-5 is involved in size-selective loosening of the endothelial barrier by cyclic AMP. *Exp. Cell Res.* **300**:202–212.

43. Bannerman, D.D., et al. 2001. A constitutive cytoprotective pathway protects endothelial cells from lipopolysaccharide-induced apoptosis. *J. Biol. Chem.* **276**:14924–14932.

44. Sawada, N., et al. 2003. Tight junctions and human diseases. *Med. Electron Microsc.* **36**:147–156.

45. Bannerman, D.D., and Goldblum, S.E. 1997. Endotoxin induces endothelial barrier dysfunction through protein tyrosine phosphorylation. *Am. J. Physiol.* **273**:L217–L226.

46. Beg, A.A., and Baltimore, D. 1996. An essential role for NF-kappaB in preventing TNF-alpha-induced cell death. *Science.* **274**:782–784.

47. Winn, R.K., and Harlan, J.M. 2005. The role of endothelial cell apoptosis in inflammatory and immune diseases. *J. Thromb. Haemost.* **3**:1815–1824.

48. Diefenbach, A., Jensen, E.R., Jamieson, A.M., and Raulet, D.H. 2001. Rae1 and H60 ligands of the NKG2D receptor stimulate tumour immunity. *Nature.* **413**:165–171.

49. Gerritsen, M.E., et al. 1995. Activation-dependent isolation and culture of murine pulmonary microvascular endothelium. *Microcirculation.* **2**:151–163.

50. Suzuki, T., Higgins, P.J., and Crawford, D.R. 2000. Control selection for RNA quantitation. *Biotechniques.* **29**:332–337.

51. Song, L., Leung, C., and Schindler, C. 2001. Lymphocytes are important in early atherosclerosis. *J. Clin. Invest.* **108**:251–259. doi:10.1172/JCI200111380.

52. Vorontchikhina, M.A., Zimmermann, R.C., Shawber, C.J., Tang, H., and Kitajewski, J. 2005. Unique patterns of Notch1, Notch4 and Jagged1 expression in ovarian vessels during folliculogenesis and corpus luteum formation. *Gene Expr. Patterns.* **5**:701–709.

53. Chiu, P.M., et al. 2006. Effect of all-trans retinoic acid on tissue dynamics of choriocarcinoma cell lines: an organotypic model. *J. Clin. Pathol.* **59**:845–850.

54. Bhattacharya, S., and Schindler, C. 2003. Regulation of Stat3 nuclear export. *J. Clin. Invest.* **111**:553–559. doi:10.1172/JCI200315372.

55. Liang, X.H., Yu, J., Brown, K., and Levine, B. 2001. Beclin 1 contains a leucine-rich nuclear export signal that is required for its autophagy and tumor suppressor function. *Cancer Res.* **61**:3443–3449.

56. Thurston, G., et al. 1999. Leakage-resistant blood vessels in mice transgenically overexpressing angiopoietin-1. *Science.* **286**:2511–2514.

57. Fridman, R., et al. 1991. Enhanced tumor growth of both primary and established human and murine tumor cells in athymic mice after coinjection with Matrigel. *J. Natl. Cancer Inst.* **83**:769–774.

58. Voronov, E., et al. 2003. IL-1 is required for tumor invasiveness and angiogenesis. *Proc. Natl. Acad. Sci. U. S. A.* **100**:2645–2650.

59. Aicher, A., et al. 2003. Essential role of endothelial nitric oxide synthase for mobilization of stem and progenitor cells. *Nat. Med.* **9**:1370–1376.

60. Yu, L., et al. 2004. Selective inactivation or reconstitution of adenosine A2A receptors in bone marrow cells reveals their significant contribution to the development of ischemic brain injury. *Nat. Med.* **10**:1081–1087.

61. Okabe, M., Ikawa, M., Kominami, K., Nakanishi, T., and Nishimune, Y. 1997. 'Green mice' as a source of ubiquitous green cells. *FEBS Lett.* **407**:313–319.